Spectroscopic Detection of Molecular Hydrogen Frozen in Interstellar Ices

Scott A. Sandford,* Louis J. Allamandola, Thomas R. Geballe

A weak infrared absorption feature near 4141 wavenumbers (2.415 micrometers) in the spectrum of WL5, an infrared source in the ρ Ophiuchus cloud complex, has been detected. It is attributed to molecular hydrogen created by irradiation and frozen in situ into water-rich ices. A second, broader absorption at 4125 wavenumbers centimeters (2.424 micrometers) is probably due to methanol in the ices. The column densities of frozen molecular hydrogen and methanol are inferred to be about 2.5×10^{18} and 3.0×10^{19}, respectively. There is about three times more frozen molecular hydrogen than frozen carbon monoxide along this line of sight.

Hydrogen in the form of H_2, the most abundant molecule in the universe, is of fundamental astrophysical importance, in part because it is the central species in all interstellar chemistry models and because it dominates the mass of clouds, thereby playing a key role in their dynamics. Most interstellar H_2 is assumed to form by H-atom recombination on dust grains in dense molecular clouds (1). Although gaseous H_2 is not expected to condense onto ice grains in appreciable quantities (2), we have recently demonstrated that it can be made and trapped within the solid state through ultraviolet photolysis of ices containing H_2O and CH_3OH (3), molecules known to be abundant in interstellar ices (4, 5). This process has an efficiency of about 10% (one H_2 produced per 10 incident photons) and can quickly saturate H_2O-rich ices with H_2 at about the 30% abundance level. [A similar production process involving cosmic rays is also possible (6)]. As a result, it is expected that many interstellar ices become saturated with H_2 on time scales that are less than or comparable to the lifetimes of typical dense molecular clouds.

Because H_2 is a homonuclear, diatomic molecule, its vibrations and rotations do not produce a change in dipole moment, making it infrared-inactive and radio-quiet. Thus, in the gas phase most H_2 is not observable by the usual astronomical techniques (7). Although thought to be widespread throughout space, H_2 is usually only detected in slightly reddened molecular clouds, shocked portions of clouds, or regions exposed to intense radiation (7, 8). However, when H_2 is frozen in a solid, its vibrational mode is perturbed by interactions with neighboring molecules. These interactions break the symmetry of the vibration, and the mode becomes weakly infrared-active (2, 9). The band strengths,

positions, and widths produced by frozen H_2 are strongly dependent on matrix composition. In the case of the interstellar medium, H_2 in the solid state would most likely be found in H_2O-rich matrices.

There are three main ways in which frozen H_2 could be present in H_2O-rich interstellar ices: (i) it could condense out of the gas phase as a pure surface layer surrounding the other ice components; (ii) it could be mixed into the ice by simultaneous codeposition with other ice-mantle components; or (iii) it could be created in situ by the energetic processing of other molecules (such as H_2O and CH_3OH) in the ices. We can rule out the first possibility because the H_2-H_2 surface binding energy is very low and pure H_2 ices are only stable in a vacuum at temperatures below about 3 K (2), colder than those typical of dense molecular clouds (10 to 40 K). The second possibility is also unlikely because the time scales for deposition of H_2O are considerably longer than the residence time of an H_2 molecule on the surface of an H_2O-rich ice mantle (3). Thus, H_2 molecules should leave the surface of interstellar ices long before they can be trapped by the deposition of successive layers of less volatile ice components. The third possibility is physically plausible, however, because it only requires that typical interstellar ices be exposed to ultraviolet or other energetic radiation, a process that is thought to occur in most dense molecular clouds.

Once trapped in an H_2O-rich ice, H_2 produces a band near 4140 cm^{-1} (2.416 μm) due to the $Q_1(1)$ pure vibrational transition (3). The full width at half maximum (FWHM) of this band is ~10 cm^{-1}. When H_2 is produced directly within the bulk of the ice by ultraviolet photolysis at 10 K, the band falls at ~4143 cm^{-1} (2.414 μm). The position of this band shifts to lower frequency as the ice is warmed, ultimately ending up near 4135 cm^{-1} (2.418 μm) at 70 K. Above 70 K the last of the H_2 escapes from the ice. A lower limit to the absorbance value (A) of this band is $A_{H_2} \geq$

$(9.4 \pm 0.9) \times 10^{-20}$ cm per molecule. Thus, if present at column densities above about 10^{18} H_2 molecules per square centimeter, solid-state H_2 should be detectable through a weak absorption band near 4140 cm^{-1} in the spectra of interstellar dense molecular clouds.

We undertook the search for frozen H_2 in space because of the potentially profound effects that substantial amounts of solid-phase H_2 could have on the physical, chemical, and dynamical properties of the ices in interstellar clouds and comets. The most promising lines of sight for its detection are those toward objects deeply embedded in cold, dense molecular clouds whose spectra contain strong absorption bands due to H_2O and CO ices. A more complete discussion of our near-infrared search for frozen H_2 and other new interstellar ice components in objects other than WL5 will be presented elsewhere (10).

Here, we report the first detection of the band shown in Fig. 1, which we attribute to H_2 frozen in H_2O-rich interstellar ices. This absorption is produced along the line of sight to WL5, an object embedded in the ρ Oph dark cloud. This cloud is part of the ρ Oph cloud complex, a region containing significant amounts of dust, ice, and gas
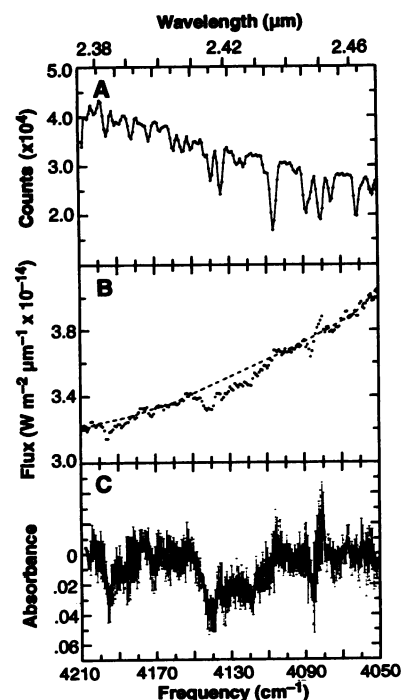

Fig. 1. The spectrum from 4210 to 4050 cm^{-1} (2.38 to 2.47 μm) of (**A**) the unratioed spectrum of the comparison star BS 5953, (**B**) the spectrum of WL5 after ratioing by BS 5953, and (**C**) the optical depth plot of WL5 derived with the continuum base line (dashed trace) shown in (B). The spectrum in (C) has been smoothed using a Gaussian with a FWHM of 1.5 data points (1/2 resolution element) and results in a resolution of ~3 cm^{-1} (19).

S. A. Sandford and L. J. Allamandola, NASA/Ames Research Center, Mail Stop 245-6, Moffett Field, CA 94035.
T. R. Geballe, Joint Astronomy Centre, Hilo, HI 96720.
*To whom correspondence should be addressed.

that block the visible light from stars within and behind the cloud. The object WL5, discovered during a 2.2-μm survey of the ρ Oph dark cloud (11), is thought to be a protostar deeply embedded in the central cluster of the cloud where the visible extinction, A_v, is at its highest ($A_v \geq 50$ magnitude) (12). The mid-infrared spectrum of WL5 contains an unusually strong 2138-cm^{-1} (4.677-μm) CO ice band with an optical depth of ~2.4 (13), an H_2O ice band at ~3300 cm^{-1} (3.0 μm) with a reported optical depth between 2.0 and 3.5 (12, 14), and evidence for a weak band near 2165 cm^{-1} (4.62 μm) (14). Both the high visible extinction and the large optical depth of the CO ice feature indicate that there is an unusually large column density of cold material between the Earth and the central parts of the ρ Oph dark cloud.

The astronomical data presented here were obtained at the United Kingdom Infrared Telescope (UKIRT) at the summit of Mauna Kea in Hawaii on the night of 20 April 1993 UT. The spectra in Fig. 1, B and C, contain two weak absorption features due to materials in the molecular cloud. The strongest (~4%) and narrowest band is centered at 4141 cm^{-1} (2.415 μm; FWHM ≈ 7 cm^{-1}). The other, broader absorption feature is weaker and is centered at ~4125 cm^{-1} (2.424 μm; FWHM ≈ 35 cm^{-1}). Other weak features in the spectra correlate with the frequencies of telluric absorption lines (Fig. 1A) and likely result from incomplete cancellation of these lines. However, the 4141-cm^{-1} band is not due to incomplete cancellation, because there is no atmospheric absorption feature at that wavelength. Examination of the unratioed spectrum of BS 5953 (Fig. 1A) indicates that neither the narrow nor the broad absorption feature is due to emission features in the comparison star. The absence of the Q(1) quadrupole line of gaseous H_2 at 4155 cm^{-1} indicates that the Q(2) line at 4143 cm^{-1} and the Q(3) line at 4126 cm^{-1} do not contribute significantly to either of the observed absorption features. Finally, these features do not appear when BS 5953 is used as the comparison star for spectra taken from other astronomical objects observed during the same night. Therefore, we conclude that the 4141- and 4125-cm^{-1} absorption features are real and associated with materials in the ρ Oph dense molecular cloud.

Figure 2 shows a comparison between the spectrum of WL5 (Fig. 1C) and the spectra of two laboratory ice analogs (3). Figure 2A compares the WL5 spectrum to that of an $H_2O{:}CH_3OH = 100{:}50$ ice analog deposited at 10 K. The CH_3OH produces a broad overtone-combination band that gives a good fit to the 4125 cm^{-1} WL5 spectral component and provides a base line for the frozen H_2 feature superposed on its high-

frequency wing. We compare the WL5 spectrum to that of an $H_2O{:}CH_3OH{:}H_2 = 100{:}50{:}\leq 10$ ice analog deposited at 15 K (Fig. 2B). The excellent match in positions, profiles, and widths of the two spectra in Fig. 2B indicates that the absorption features shown in Fig. 1C are due to H_2 and CH_3OH frozen into H_2O-rich ices in the ρ Oph dense molecular cloud.

The position of the astronomical H_2 feature can be used to estimate the temperature of the interstellar ices containing the H_2 (3). The best fit is found for ices in which the H_2 is formed in situ through ultraviolet photolysis at low temperatures and warmed to ~15 to 30 K. This temperature range is compatible with the dust temperatures expected in the denser parts of molecular clouds (10 to 40 K). In the optically thin case, the column densities (N_i, in molecules per square centimeter) of the various ice components can be derived from

$$N_i = \frac{\int \tau_i(v)dv}{A_i} \approx \frac{\tau_{imax}\Delta v_{1/2}}{A_i} \qquad (1)$$

where $\tau_i(v)$ is the optical depth of an absorption band due to component i as a function of frequency, τ_{imax} is the optical depth of the band at its deepest point, A_i is the integrated absorbance of the band in
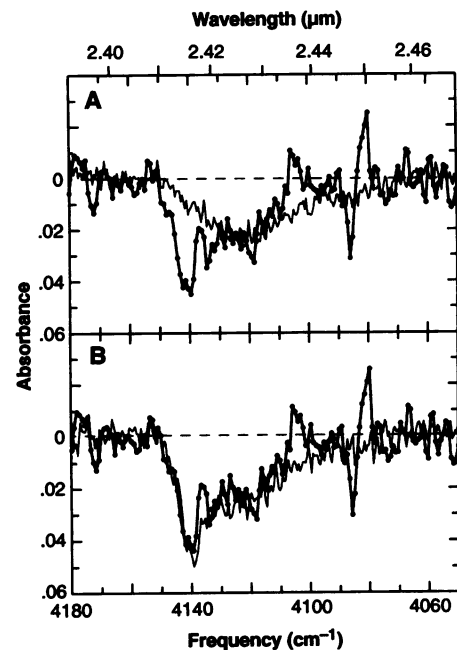

Wavelength (μm)

Fig. 2. A comparison between the optical depth spectra of WL5 (thick trace with points) and two laboratory interstellar ice analogs (thin traces) (3). (A) WL5 compared with an $H_2O{:}CH_3OH = 100{:}50$ ice deposited at 10 K and (B) WL5 compared with an $H_2O{:}CH_3OH{:}H_2 = 100{:}50{:}10$ ice deposited at 15 K. The narrower absorption near 4141 cm^{-1} (2.415 μm) is due to H_2 frozen in interstellar H_2O-rich ices. The broader absorption feature near 4125 cm^{-1} (2.424 μm) is due to CH_3OH in the ices.

centimeters per molecule, and $\Delta v_{1/2}$ is the band's FWHM. From Fig. 2A we measure $\tau_{CH_3OHmax} = 0.02$ and $\Delta v_{1/2CH_3OH} = 30$ cm^{-1}. Using the CH_3OH band in the laboratory spectrum as a base line for the H_2 feature, we measure $\tau_{H_2max} = 0.032$ and $\Delta v_{1/2H_2} = 7$ cm^{-1}. Using $A_{CH_3OH}(4125$ cm$^{-1}) = 2 \times 10^{-20}$ cm per molecule (15) and the lower limit of $A_{H_2}(4140$ cm$^{-1}) \geq 9 \times 10^{-20}$ cm per molecule (3), we derive solid-state column densities toward WL5 of $N_{CH_3OH} = 3.0 \times 10^{19}$ cm^{-2} and $N_{H_2} \leq 2.5 \times 10^{18}$ cm^{-2}, yielding $H_2/CH_3OH \leq 0.08$. These values can be compared to those associated with other ice components along the same line of sight. For CO, a column density of 7.6×10^{17} cm^{-2} is derived from $\tau_{COmax} = 2.4$, $\Delta v_{1/2CO} = 3.8$ cm^{-1} (14), and $A_{CO}(2138$ cm$^{-1}) = 1.2 \times 10^{-17}$ cm per molecule (16). This value for N_{CO} is probably a lower limit because the CO band is partially saturated. Thus, $CH_3OH{:}CO{:}H_2 \approx 100{:}3{:}8$, values that fall within anticipated ranges (3). The column density of H_2O ice is not considered here, as it is much less certain (12, 13) because of the extensive depth of the H_2O band and the unknown extent of saturation effects.

We have detected two new absorption bands at 4141 and 4125 cm^{-1} in the spectrum of WL5 that indicate the presence of H_2 and CH_3OH frozen into H_2O-rich ices in the ρ Oph dense molecular cloud. The H_2 band position suggests that the H_2 was produced in situ, probably as the result of irradiation of 15- to 30-K interstellar ices by ultraviolet photons, cosmic rays, or both. While the abundance of solid-state H_2 relative to H_2O is uncertain, previous laboratory studies of H_2-containing ices and the detection reported here suggest that at grain temperatures below 70 K, H_2 produced by ultraviolet or cosmic rays could represent an important component of typical interstellar ices. The presence of H_2 in grain mantles should have significant effects on the physical properties and chemistry of the ices in dense molecular clouds and in comets. For example, laboratory work indicates that H_2O-rich interstellar ices saturate in H_2 at ratios near $H_2/H_2O = 0.3$ (3), a concentration at which guest molecules begin to interfere seriously with the ability of H_2O to form a completely H-bonded lattice (17). The total intermolecular binding energy (ΔH_s) of an $H_2O{:}H_2 = 100{:}30$ ice should be about 1.6 times less than that of a comparable pure H_2O ice (16). Because the rate of sublimation varies as $e^{-\Delta H_s}$, the presence of large amounts of H_2 in these ices should significantly enhance the rate at which condensed species are injected back into the gas phase by grain sublimation (15) and disruption processes (6, 18). Furthermore, because comets may contain relatively unaltered interstellar dust and ices, the

presence of H_2 could contribute to cometary activity at large heliocentric distances. Finally, the H_2 may also have significant effects on the chemistry associated with the gas and solid phases in these environments. Ultimately, the importance of frozen H_2 will depend on its ubiquity in space. Although difficult, the detection of the 4141-cm^{-1} H_2 feature along additional lines of sight, especially those having more normal, smaller column densities, is clearly of importance.

REFERENCES AND NOTES

1. D. Hollenbach and E. E. Salpeter, *J. Chem. Phys.* **53**, 79 (1970); *Astrophys. J.* **163**, 155 (1971); D. R. Flower and G. Pineau des Forets, *Mon. Not. R. Astron. Soc.* **247**, 500 (1990).
2. H. C. van de Hulst, *Rech. Astron. Obs. Utrecht* **11**, 1 (1949); T. J. Lee, L. Gowland, V. C. Reddish, *Nature Phys. Sci.* **231**, 193 (1971); T. J. Lee, *ibid.* **237**, 99 (1972); G. N. Brown and W. T. Ziegler, *Adv. Cryog. Eng.* **25**, 662 (1980); P. C. Souers, *Hydrogen Properties for Fusion Energy* (Univ. of California Press, Berkeley, 1986).
3. S. A. Sandford and L. J. Allamandola, *Faraday Symposium No. 28*, "Chemistry in the Interstellar Medium," Birmingham, England, 16 to 18 December 1992 (Royal Society of Chemistry, London, 1992); *Astrophys. J. Lett.* **409**, L65 (1993).
4. L. J. Allamandola and S. A. Sandford, in *Dust in the Universe*, M. E. Bailey and D. A. Williams, Eds. (Cambridge Univ. Press, Cambridge, 1988), p. 229.
5. _____, A. Tielens, T. M. Herbst, *Astrophys. J.* **399**, 134 (1992).
6. V. Pironello and D. Averna, *Astron. Astrophys.* **196**, 201 (1988); R. Hudson and M. Moore, *J. Phys. Chem.* **96**, 6500 (1992).
7. J. M. Shull and S. Beckwith, *Annu. Rev. Astron. Astrophys.* **20**, 163 (1982).
8. P. W. J. L. Brand, *J. Chem. Soc. Faraday Trans.* **89**, 2131 (1993).
9. J. De Remigis and H. L. Welsh, *Can. J. Phys.* **48**, 1622 (1970); G. R. Smith *et al.*, *J. Chem. Phys.* **65**, 1591 (1976); J. A. Warren, G. R. Smith, W. A. Guillory, *ibid.* **72**, 4901 (1980).
10. S. A. Sandford, T. R. Geballe, L. J. Allamandola, in preparation.
11. B. A. Wilking and J. L. Lada, *Astrophys. J.* **274**, 698 (1983).
12. M. Tanaka, S. Sata, T. Nagata, T. Yamamoto, *ibid.* **352**, 724 (1990).
13. T. H. Kerr, A. J. Adamson, D. C. B. Whittet, *Mon. Not. R. Astron. Soc.* **251**, 60p (1991).
14. _____, in preparation.
15. S. A. Sandford and L. J. Allamandola, *Astrophys. J.*, in press.
16. D. M. Hudgins *et al.*, *Astrophys. J. Suppl. Ser.* **86**, 713 (1993).
17. W. Hagen, A. Tielens, J. M. Greenberg, *Astron. Astrophys. Suppl. Ser.* **51**, 389 (1983).
18. L. B. d'Hendecourt, L. J. Allamandola, F. Baas, J. M. Greenberg, *Astron. Astrophys.* **109**, L12 (1982); W. A. Schutte and J. M. Greenberg, *ibid.* **244**, 190 (1991).
19. Spectra were taken with CGS4, a cryogenic grating, two-dimensional InSb array spectrometer, capable of covering the 1- to 5-μm wavelength region at resolving powers between 200 and 20,000. These spectra of WL5 and a nearby comparison star (BS 5953) were obtained with a 150-groove-per-millimeter grating in second order, which provided a resolving power of ~1550 (Δv = 2.7 cm^{-1} and $\Delta\lambda$ = 0.0016 μm, where λ is the wavelength). The wavelength setting of the grating was calibrated with a xenon emission-line lamp and is accurate to ~0.2 cm^{-1} (0.0001 μm; 1 SD). The total integration time on WL5 was 20 min. Individual 1-min integrations were normalized to the scan with the highest number of counts. None of the 19 individual integrations used in the co-added data had counts lower than 94% of the maximum integration period, and most were within 98 to 99% of the maximum. To calibrate flux and remove the effects of atmospheric absorption, we ratioed the spectrum of WL5 against that of BS 5953 (Fig. 1, A and B), which was assumed to have a K wave band magnitude of 3.12 and a blackbody temperature of 24,500 K. The spectrum of BS 5953 was taken directly before that of WL5, and the average air masses of the two observations agree to within 0.01 of an air mass. Despite this close agreement in air mass, small residual spectral features due to incomplete cancellation of atmospheric H_2O lines were apparent in the original ratioed data. These features were partially removed by the scaling of the comparison star data by a small factor before reduction. The base line given by the dashed line in Fig. 1B was then used to derive the optical depth plot given in Fig. 1C.
20. We thank the staff of UKIRT, which is operated by the Royal Observatory Edinburgh on behalf of the U.K. Science and Engineering Research Council, for its support of these observations. Supported also by National Aeronautics and Space Administration grants 452-33-93-03 (Origins of Solar Systems Program) and 199-52-12-04 (Exobiology Program).

Closely Approaching the Silylium Ion (R3Si+)

Christopher A. Reed,* Zuowei Xie, Robert Bau, Alan Benesi

The crystal structure of the tri-isopropyl silyl species, i-Pr$_3$Si(Br$_6$-CB$_{11}$H$_6$), where the brominated carborane Br$_6$-CB$_{11}$H$_6^-$ is perhaps the least nucleophilic anion presently known, has revealed the highest degree of silylium cation character (R$_3$Si$^+$) yet observed. The average C–Si–C angle is 117°, only 3° short of the planarity expected of a pure silylium ion (120°). This value compares to 114° recently reported for a toluene-solvated silyl cation, [Et$_3$Si(toluene)]$^+$ by Lambert and co-workers. The greater silylium ion character of i-Pr$_3$Si(Br$_6$-CB$_{11}$H$_6$) versus [i-Pr$_3$Si(toluene)]$^+$ is also reflected in the larger downfield shift of the silicon-29 nuclear magnetic resonance, 109.8 versus ≤94.0 parts per million. The unusual bonding of toluene to R$_3$Si$^+$ in Lambert's compound is reinterpreted as a significant covalent π interaction.

There has been recent progress in the long search for a three-coordinate silicon cation (R$_3$Si$^+$, silylium ion) analogous to widely known carbocations (R$_3$C$^+$). Lambert *et al.* (1) have determined the crystal structure of the triethylsilyl cation with no coordination of the anion and weak coordination of the solvent (toluene). Indeed, the coordination of toluene with a long Si–C distance of 2.18 Å is unprecedented in silicon chemistry. It is not, however, unprecedented in silver chemistry. In a so-called η^1-benzene complex of silver(I), a similar π-complexation of an arene solvent molecule has been observed and structurally characterized (2). The silver ion in Ag(benzene)(CB$_{11}$H$_{12}$) sits almost directly over one carbon atom of the benzene ring at an Ag–C distance of 2.40 Å. This π-bonding distance is ~0.2 Å longer than typical Ag–C σ bonds (2.13 to 2.25 Å) (3). The 2.18 Å Si–C distance to toluene in [Et$_3$Si(toluene)]$^+$ (Et, ethyl) is ~0.3 Å longer than a typical average Si–C σ bond, ~1.87 Å (ranging from 1.80 to 2.03 Å) (4). We therefore conclude that the Si–C bond in [Et$_3$Si(toluene)]$^+$ is close to what should be expected for π-arene coordination to silicon.

The reality and significance of this co-

valent bonding is reflected in the pyramidalization of the triethylsilyl moiety. The average C–Si–C angle of the σ bonds in [Et$_3$Si(toluene)]$^+$ is 114°, well short of the 120° expected of a discrete sp^2 R$_3$Si$^+$ ion and is, in fact, comparable to other solvent-coordinated species such as [i-Pr$_3$Si(acetonitrile)]$^+$ (115°) (i-Pr, isopropyl) (5). Although there is good reason to expect planar R$_3$Si$^+$ to be readily deformable, particularly with bulky ligands like π-arenes, to suggest that covalent bonding may be absent and that the silicon is essentially three-coordinate (1, 6) overstates the case. Nevertheless, the structure has important novelty as a model for intermediates in electrophilic aromatic substitution, particularly since one might have expected a σ-type structure (known as a "Wheland intermediate") like that observed in the heptamethylbenzenium ion (7). Of the two idealized contributing resonance structures indicated below, a π-complex with sp^2 carbon and a σ-complex with sp^3 carbon, the best single description is as a π-complex.
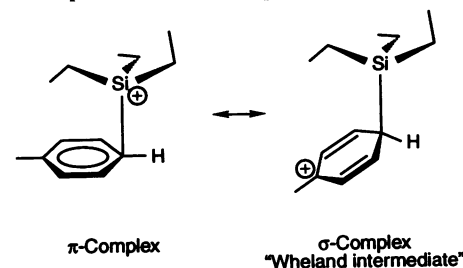
C. A. Reed, Z. Xie, R. Bau, Department of Chemistry, University of Southern California, Los Angeles, CA 90089–0744.
A. Benesi, Department of Chemistry, Pennsylvania State University, University Park, PA 18602.

*To whom correspondence should be addressed.

π-Complex

σ-Complex
"Wheland intermediate"